Biophysical Chemistry 10 (1979) 203–210

ISOELECTRIC FOCUSING OF INTERACTING SYSTEMS. IV. INTERACTION OF MACROMOLECULES WITH EACH OTHER AND WITH LIGANDS *

John R. CANN and Katheleen J. GARDINER
Department of Biophysics and Genetics, University of Colorado Medical Center, Denver, Colorado 80262, USA

Received 20 March 1979

The theoretical isoelectric focusing behavior for rapidly reversible, bimolecular complexing between two macromolecules depends upon the relative value of the isoelectric point of the complex. When it is intermediate in value, the transient patterns exhibit three peaks. As equilibrium is approached the central peak of complex disappears leaving two reactant peaks. When the isoelectric point is acidic or alkaline to both reactants, the equilibrium pattern also shows two peaks; but in this case only one is pure reactant, the other being a reaction zone. The two cases can be distinguished by varying the relative amounts of reactants. Transient patterns for ligand-binding exhibit a peak of unliganded protein and a reaction zone. As the charged ligand is driven out of the focusing column the reaction zone disappears, so that the equilibrium pattern shows only a peak of unliganded protein. In general, the isoelectric point of the complex cannot be determined from the transient patterns.

1. Introduction

Recently [1–4] we have formulated a phenomenological theory of isoelectric focusing for systems undergoing rapidly reversible, carrier ampholyte-induced macromolecular isomerization or association-dissociation reactions, or pH-dependent conformational transitions. The calculations predict that such interactions can give well-resolved bimodal (for certain reaction schemes multimodal) focusing patterns in which the peaks correspond to different equilibrium compositions and not to separated macromolecular species. This prediction is confirmed experimentally by several reports [5–11] of isoelectric focusing patterns which exhibit two or more peaks due to reversible interactions as ascertained by fractionation experiments. Thus, the implications of these new insights for conventional analytical and preparative isoelectric focusing are evident. The same concepts are also relevant to the application of isoelectric focusing in fundamental studies on biochemical reactions such as protein-drug interactions, interaction of enzymes with coenzymes and allosteric affectors, and the interaction of macromolecules with each other. Preliminary findings [12–15] indicate that isoelectric focusing holds promise for the study of such interactions. Our objective in this paper and in the accompanying communication [16] is to expand the theoretical basis for this application of the method.

Two classes of rapidly equilibrating reactions are considered in this paper: Formation of a bimolecular complex, $\mathcal{C}$, between two amphoteric macromolecules, $\mathcal{A}$ and $\mathcal{B}$, with different isoelectric points (pI_i)

$$\mathcal{A} + \mathcal{B} \rightleftharpoons \mathcal{C}, \quad K_1 , \tag{1}$$

and the binding of a charged ligand molecule, $\mathcal{L}$, by a protein, $\mathcal{P}$,

$$\mathcal{P} + \mathcal{L} \rightleftharpoons \mathcal{PL}, \quad K_2 . \tag{2}$$

In the case of reaction (1), calculations have been made for both $pI_{\mathcal{A}} < pI_{\mathcal{C}} < pI_{\mathcal{B}}$ and $pI_{\mathcal{C}} < pI_{\mathcal{A}} < pI_{\mathcal{B}}$. For reaction (2), it is assumed that $pI_{\mathcal{PL}} < pI_{\mathcal{P}}$ and that the negative charge on the ligand is constant over

* Supported in part by Research Grant 5R01 HL13909-27 from the National Heart, Lung, and Blood Institute, National Institutes of Health, U.S. Public Health Service. This publication is No. 730 from the Department of Biophysics and Genetics, University of Colorado Medical Center, Denver, Colorado 80262.

the pH range of interest. Aside from the dependence of the electrophoretic velocities of the macromolecular species upon pH, neither reaction is coupled to the pH gradient or the distribution of carrier ampholytes along the isoelectric focusing column. This is a simplification for some systems. Since the macromolecular reactants and products have different pI's, the pK's of certain ionizable groups may be altered upon reaction. In that event, the "equilibrium constant", K_i, would have to incorporate the pK's of reactant(s) and product in such a way as to be a function of hydrogen ion concentration. We assume that the "equilibrium constant" would be an insensitive function of pH, in which case it could be considered constant in the region of the column where the particular system focuses, given the shallow pH gradient and the relatively small difference(s) in pI's.

2. Theory

Transient isoelectric focusing patterns have been computed by numerical solution of the simultaneous transport equations and mass action expressions as a function of time, t, thereby constructing the approach to the equilibrium pattern. The calculations are essentially as described previously [1] except for the following two modifications: (1) The appropriate mass action expressions are used for recalculation of chemical equilibrium after each time cycle of diffusion and driven transport. (2) The boundary conditions for the macromolecular species correspond to reflection of the molecules at the ends of the isoelectric focusing column in order to assure good material balance (to better than 4.5×10^{-4}%) in the relatively short (1.5 cm) column. This expediency does not cause any significant accumulation of material at either end of the column. The boundary conditions for unbound ligand constitute a sink at each end.

In the case of reaction (1) most of the calculations are for a broad (1.1 cm) initial zone of chemically equilibrated macromolecules encompassing the pI's. The others are for a narrow zone (0.1 cm) containing the same quantities of constituent macromolecules and situated anodically to the pI's. For reaction (2) the initial condition is generally a narrow zone of an equilibrated mixture of macromolecule and ligand, positioned either cathodically or anodically to the pI's. While the equilibrium pattern is independent of initial conditions, the time-course of approach to equilibrium may differ. As discussed earlier [1] the calculations for the broad initial zone can be placed into correspondence with the experimental procedure in which both macromolecule and carrier ampholytes are distributed uniformly throughout the isoelectric focusing column initially. The narrow initial zone simulates the procedure in which a small sample is inserted into the preformed pH gradient.

The calculations were made on the University of Colorado's CDC 6400 computer. The values of the several parameters are as follows: $\Delta x = 0.01$ cm; $\Delta t = 5$ s; equal molecular weights for $\mathcal{A}$ and $\mathcal{B}$ in reaction (1); diffusion coefficients of $\mathcal{A}$, $\mathcal{B}$ and $\mathcal{C}$, 7.6×10^{-7}, 7.6×10^{-7} and 6.0×10^{-7} cm^2 s^{-1}, respectively; diffusion coefficients of $\mathcal{P}$, $\mathcal{PL}$ and $\mathcal{L}$ in reaction (2), 7.6×10^{-7}, 6×10^{-7} and 1×10^{-5} cm^2 s^{-1}, respectively; driven velocity of macromolecular species i, $V_i(x) = 10^{-4}(a_i - x)$, in which x is the position in the isoelectric focusing column and a_i is the location of pI_i indicated in each of the figures by a vertical arrow for the designated species; halving the electric field strength halves the numerical coefficient in $V_i(x)$; values of constant driven velocity of $\mathcal{L}$ in reaction (2), $V_{\mathcal{L}} = -2.5 \times 10^{-4}$ or -5×10^{-4} cm s^{-1}, as given in legends to appropriate figures.

The computed isoelectric focusing patterns are displayed as plots of the molar constituent concentration of macromolecule (viz, $\bar{C} = C_{\mathcal{A}} + C_{\mathcal{CB}} + 2C_{\mathcal{C}}$ for reaction (1) and $\bar{C} = C_{\mathcal{P}} + C_{\mathcal{PL}}$ for reaction (2)) against x with the anode to the left. In several instances the concentrations of individual macromolecular species (C_i) and, in the case of reaction (2), unbound ligand ($C_{\mathcal{L}}$) are also shown. Initial constituent concentrations of reactants are designated as $\bar{C}^0_{\mathcal{A}}$, $\bar{C}^0_{\mathcal{CB}}$, $\bar{C}^0_{\mathcal{C}}$ and $\bar{C}^0_{\mathcal{L}}$.

3. Results

Reaction (1), $pI_{\mathcal{A}} < pI_{\mathcal{C}} < pI_{\mathcal{CB}}$. Representative isoelectric focusing patterns computed for Reaction 1 for the case in which the pI of the complex is intermediate between those of the two interacting macromolecules, are presented in figs. 1–3. The patterns in figs. 1 and 2 are for $\bar{C}^0_{\mathcal{A}} = \bar{C}^0_{\mathcal{CB}}$, while those in fig. 3 are for $\bar{C}^0_{\mathcal{A}} = 2\bar{C}^0_{\mathcal{CB}}$. The transient patterns characteristically exhibit three peaks, a central peak composed largely of

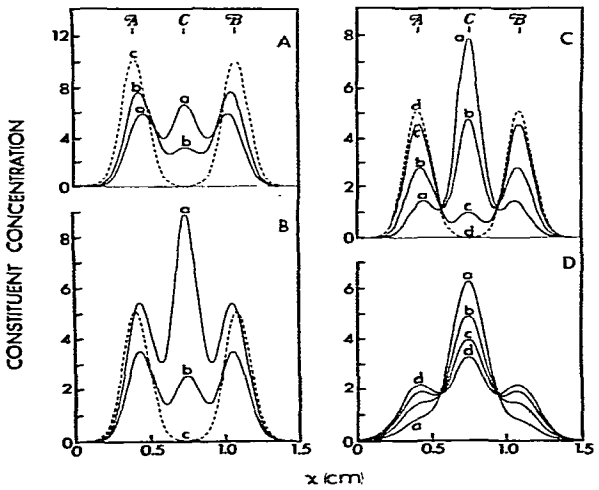

Fig. 1. Theoretical isoelectric focusing patterns calculated for reaction (1) with $pI_{\mathcal{A}} < pI_{\mathcal{C}} < pI_{\mathcal{B}}$. A – Time course of approach to equilibrium for $K_1 = 4 \times 10^4\ M^{-1}$ and $\bar{C}^0_{\mathcal{A}} = \bar{C}^0_{\mathcal{B}} = 2 \times 10^{-4}$ M: a, $t = 3 \times 10^4$ s; b, 4×10^4 s; c, 1×10^5 s. B – Dependence of the shape of the pattern upon initial constituent concentrations at constant $t = 5 \times 10^4$ s for $K_1 = 2 \times 10^5\ M^{-1}$: a, $\bar{C}^0_{\mathcal{A}} = \bar{C}^0_{\mathcal{B}} = 2 \times 10^{-4}$ M; b, 1×10^{-4} M; c, 1×10^{-5} M. C – Time-course of approach to equilibrium for $K_1 = 2 \times 10^7\ M^{-1}$ and $\bar{C}^0_{\mathcal{A}} = \bar{C}^0_{\mathcal{B}} = 1 \times 10^{-5}$ M: a, $t = 5 \times 10^4$ s; b, 1×10^5 s; c, 2×10^5 s; d, 3×10^5 s. D – Same as C except that the electric field strength is halved: a, $t = 1 \times 10^5$ s; b, 2×10^5 s; c, 3×10^5 s; d, 4×10^5 s. Ordinates: fig. 1A, $10^4 \times \bar{C}$; fig. 1B, $10^4 \times \bar{C}$ for curves a and b and $10^5 \times \bar{C}$ for curve c; figs. 1C and 1D, $10^5 \times \bar{C}$. The results present in this figure and figs. 2–4 are for a broad initial zone.

complex and focused at its pI flanked by two peaks proximate to the pI's of the reactants. As time goes on, the flanking peaks grow progressively in size at the expense of the central one until at equilibrium the pattern exhibits only two non-overlapping peaks focused at the pI's of the reactants. In other words, at equilibrium, all of the complex is dissociated into two reactant peaks, each of which is pure. This behavior is shown even by relatively weak interactions provided that the initial constituent concentrations of reactants are sufficiently high, fig. 1A. The dependence of the shape of the pattern upon concentration at constant time of focusing is illustrated in fig. 1B which shows that the lower the concentration, the more rapid is the approch to equilibrium. Moreover, at the lowest concentration the transient patterns exhibit only two peaks even during early stages of focusing; i.e., under these

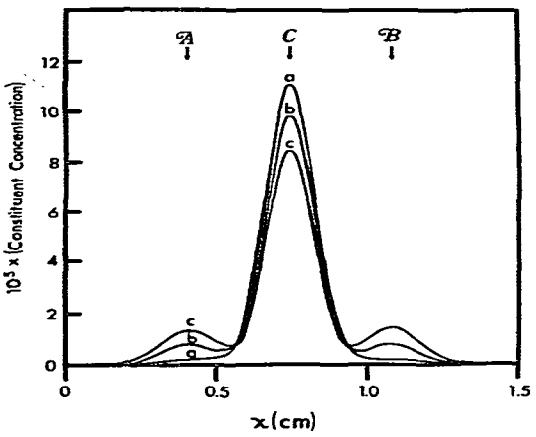

Fig. 2. Isoelectric focusing patterns for reaction (1), $pI_{\mathcal{A}} < pI_{\mathcal{C}} < pI_{\mathcal{B}}$, with $\bar{C}^0_{\mathcal{A}} = \bar{C}^0_{\mathcal{B}} = 1 \times 10^{-5}$ M and $K_1 = 2 \times 10^9\ M^{-1}$: a, $t = 5 \times 10^4$ s; b, 2×10^5 s; c = 4×10^5 s. The pattern for $K_1 = 2 \times 10^{11}\ M^{-1}$ at $t = 3 \times 10^5$ s is virtually the same as curve a.

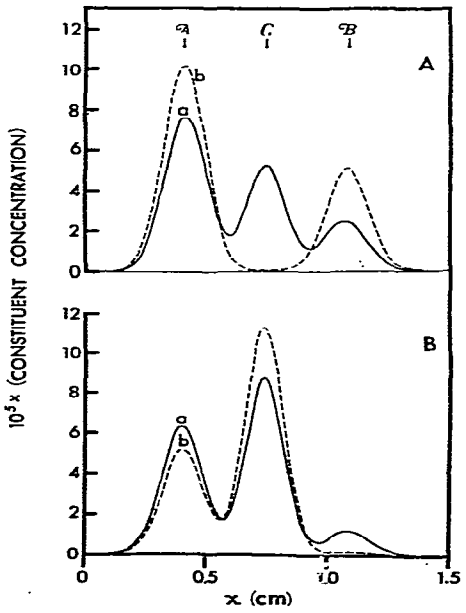

Fig. 3. Isoelectric focusing patterns for reaction (1), $pI_{\mathcal{A}} < pI_{\mathcal{C}} < pI_{\mathcal{B}}$, with $\bar{C}^0_{\mathcal{A}} = 2 \times 10^{-5}$ M and $\bar{C}^0_{\mathcal{B}} = 1 \times 10^{-5}$ M. A – $K_1 = 2 \times 10^7\ M^{-1}$: a, $t = 1 \times 10^5$ b, 3×10^5 s. B – a, $K_1 = 2 \times 10^9\ M^{-1}$ and $t = 4 \times 10^5$ s; b, $2 \times 10^{11}\ M^{-1}$ and 2×10^5 s.

conditions the dynamics of focusing are as if the reactants were noninteracting. However, increasing the strength of the interaction (i.e., increasing K_1) while holding the initial constituent concentrations at this low value, results once again in transient patterns exhibiting three peaks with a corresponding decrease in the rate of approach to equilibrium. (Compare pattern c in fig. 1B with those in figs. 1C and 2). For sufficiently large K_1 the rate of approach is so slow that, for all practical times of operation, the pattern shows virtually a single peak focussed at the pI of the complex, but of course, containing unbound reactants at very low concentration.

The slow rate of approach to equilibrium can not be due to intrinsically slow dissociation of the complex since we have assumed instantaneous establishment of chemical equilibrium during the focusing process. The explanation is provided by the effect of electric field strength, E. Comparison of figs. 1C and 1D reveals that lowering the field strength decreases the rate of approach, the half-time of disappearance of the central peak varying inversely with E^2. The conclusion reached is that the rate-controlling factor is the electrical power input ($P = E^2 \kappa l/A$, where κ is the specific conductance; l, the length of the column, and A, its cross-sectional area). The power input supplies the free energy of dissociation of the complex. Mechanistically, the electrical work is used to drive unbound reactants out of the central peak toward their respective pI's with accompanying and progressive dissociation of the complex as a result of mass action. The process continues until all of the complex is dissociated and the reactants completely separated by being focused at their pI's. This explanation accounts for the dependence of the rate of approach to equilibrium upon both the initial constituent concentrations and the strength of interaction, which exert their effects via the role of mass action in the mechanism.

The foregoing results are for $\bar{C}^0_{\mathcal{A}} = \bar{C}^0_{\mathcal{B}}$, but in practice one of the reactants might be in excess. The isoelectric focusing patterns presented in fig. 3 for $\bar{C}^0_{\mathcal{A}} = 2\bar{C}^0_{\mathcal{B}}$ illustrate both the variety of patterns one can anticipate and the fact that the dynamics of focusing are essentially the same as described above.

These several calculations are for a broad initial zone. Exploratory calculations for a narrow initial zone positioned anodically to the pI's gave essentially the same patterns as displayed in fig. 1C for the same value of K_1.

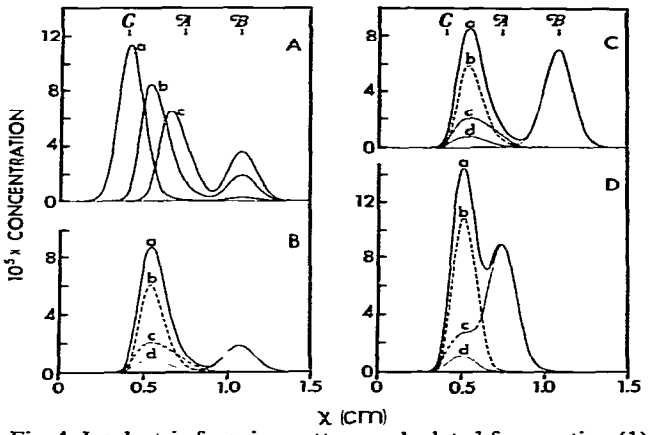

Fig. 4. Isoelectric focusing patterns calculated for reaction (1) with $pI_{\mathcal{C}} < pI_{\mathcal{A}} < pI_{\mathcal{B}}$. A – Dependence of the shape of the pattern at 4×10^5 s upon the value of K_1 for $\bar{C}^0_{\mathcal{A}} = \bar{C}^0_{\mathcal{B}} = 1 \times 10^{-5}$ M: a, $K_1 = 2 \times 10^7\ M^{-1}$; b, $2 \times 10^5\ M^{-1}$; c, $5 \times 10^4\ M^{-1}$. B – Pattern at 4×10^5 s for $K_1 = 2 \times 10^5\ M^{-1}$ and $\bar{C}^0_{\mathcal{A}} = \bar{C}^0_{\mathcal{B}} = 1 \times 10^{-5}$ M showing distribution of $\bar{C}$ (curve a), $2C_{\mathcal{C}}$ (curve b), $C_{\mathcal{A}}$ (curve c) and $C_{\mathcal{B}}$ (curve d). C – Same as B except that $\bar{C}^0_{\mathcal{A}} = 1 \times 10^{-5}$ M and $\bar{C}^0_{\mathcal{B}} = 2 \times 10^{-5}$ M. D – Same as B except that $\bar{C}^0_{\mathcal{A}} = 3 \times 10^{-5}$ M and $\bar{C}^0_{\mathcal{B}} = 1 \times 10^{-5}$ M (3×10^5 s).

Reaction (1), $pI_{\mathcal{C}} < pI_{\mathcal{A}} < pI_{\mathcal{B}}$. The isoelectric focusing behavior for this case is in sharp contrast to that just described for $pI_{\mathcal{A}} < pI_{\mathcal{C}} < pI_{\mathcal{B}}$. Thus, the transient as well as the equilibrium patterns show only two peaks and, as we shall see shortly, only one of the peaks corresponds to pure reactant.

The patterns displayed in fig. 4 are, for all practical purposes, equilibrium patterns as judged by the criterium that the following quantities remain constant to four places with a maximum change of only two parts in the fifth place between 3×10^5 and 4×10^5 sec of focusing: $\bar{C}$ at each position in the pattern; amoung of each species in the pattern; and the mean position and second moment about the mean of the distribution of $\bar{C}$ and each of the species.

The patterns for $\bar{C}^0_{\mathcal{A}} = \bar{C}^0_{\mathcal{B}}$ (fig. 4A) show a major peak located between $pI_{\mathcal{C}}$ and $pI_{\mathcal{A}}$ at a position depending upon the value of K_1 and a minor peak focused at $pI_{\mathcal{B}}$. As shown in fig. 4B the major peak is a reaction zone containing $\mathcal{A}$, $\mathcal{B}$ and $\mathcal{C}$ at chemical equilibrium and focused at the constituent pI of the mixture ($p\bar{I}$), while the minor peak corresponds to pure $\mathcal{B}$. The bimodal distribution of $\mathcal{B}$ through the pattern is particularly noteworthy. The $p\bar{I}$ of the reac-

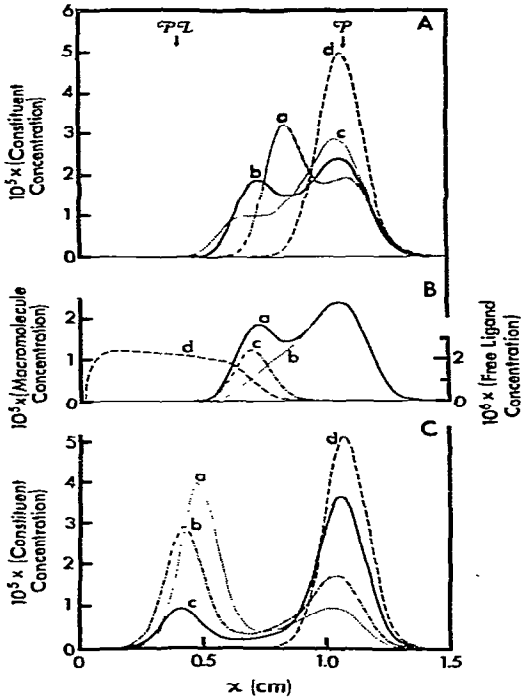

Fig. 5. Theoretical isoelectric focusing patterns calculated for reaction (2), negatively charged ligand and $pI_{\mathcal{PL}} < pI_{\mathcal{P}}$. A – Time-course of approach to equilibrium for $K_2 = 2 \times 10^6$ M^{-1}, $\bar{C}^0_{\mathcal{L}} = \bar{C}^0_{\mathcal{P}} = 1.0091 \times 10^{-4}$ M and $V_{\mathcal{L}} = -2.5 \times 10^{-4}$ cm s^{-1}: a, $t = 8 \times 10^3$ s; b, 1.2×10^4 s; c, 1.6×10^4 s; d, 4×10^4 s; equilibrium is reached at 4×10^5 s by which time the single peak has focused at $pI_{\mathcal{P}}$. B – Pattern b of A showing distribution of $\bar{C}$ (curve a), $C_{\mathcal{P}}$ (curve b), $C_{\mathcal{PL}}$ (curve c) and $C_{\mathcal{L}}$ (curve d). C – Time-course of approach to equilibrium for $K_2 = 2 \times 10^8$ M^{-1}, $\bar{C}^0_{\mathcal{L}} = \bar{C}^0_{\mathcal{P}} = 1.0091 \times 10^{-4}$ M and $V_{\mathcal{L}} = -5.0 \times 10^{-4}$ cm s^{-1}: a, $t = 2.4 \times 10^4$ s; b, 4×10^4 s, c, 8×10^4 s; d, 1.6×10^5 s. These results are for a narrow initial zone positioned cathodically to the pI's.

tion zone drifts towards $pI_{\mathcal{A}}$ with decreasing value of K_1 because, as the strength of interaction decreases, the concentration of $\mathcal{C}$ in the zone also decreases with concomitant increase in $\mathcal{A}$ and $\mathcal{B}$. The nature of the pattern remains essentially unchanged when $\bar{C}^0_{\mathcal{B}}$ is increased at constant $\bar{C}^0_{\mathcal{A}}$ and K_1 (fig. 4C), the main consequence being an increase in the size of the peak of $\mathcal{B}$. On the other hand, increasing $\bar{C}^0_{\mathcal{A}}$ at constant $\bar{C}^0_{\mathcal{B}}$ has a major effect on the profile (fig. 4D). The pattern still shows the reaction zone, but the peak focused at $pI_{\mathcal{B}}$ has disappeared and is replaced by a peak of pure $\mathcal{A}$ focused at its pI. The distribution of $\mathcal{B}$ is now unimodal, while the distribution of $\mathcal{A}$ shows a

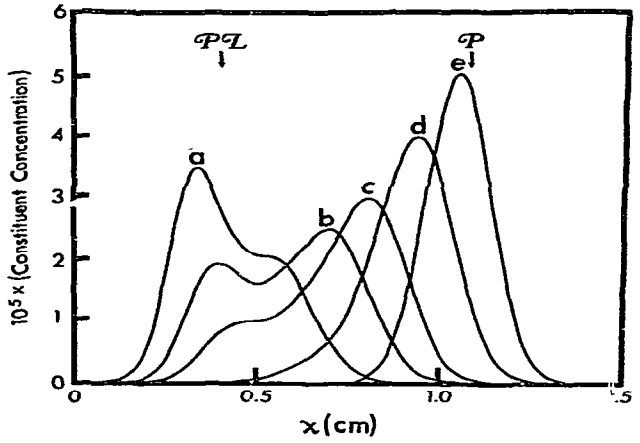

Fig. 6. Isoelectric focusing patterns for reaction (2) with $K_2 = 2 \times 10^6 M^{-1}$, $\bar{C}^0_{\mathcal{L}} = 1.0091 \times 10^{-3}$ M, $\bar{C}^0_{\mathcal{P}} = 1.0091 \times 10^{-4}$ M, $V_{\mathcal{L}} = -2.5 \times 10^{-4}$ cm s^{-1} and a narrow initial zone positioned anodically to the pI's: a, $t = 8 \times 10^3$ s; b, 1.2×10^4 s; c, 1.6×10^4 s; d, 2.4×10^4 s; e, 4×10^4 s. The results of control calculations for a narrow initial zone cathodic to the pI's are the same as in fig. 5A except for a small translation of the bimodal patterns towards the anode and a somewhat slower approach to equilibrium.

major peak with a strong shoulder embodied in the reaction zone.

This behavior can be understood mechanistically as follows: As the electric field drives $\mathcal{A}$ and $\mathcal{B}$ out of the region of the isoelectric focusing column between $pI_{\mathcal{C}}$ and $pI_{\mathcal{A}}$ in the same direction toward their respective pI's, they continuously interact to form $\mathcal{C}$ which, in turn, is driven back in the direction of its pI. Thus, the origin of the reaction zone. For $\bar{C}^0_{\mathcal{A}} \leqslant \bar{C}^0_{\mathcal{B}}$ some of the faster migration $\mathcal{B}$ can escape to its pI, but the reaction prevents formation of a peak of pure $\mathcal{A}$. When $\bar{C}^0_{\mathcal{A}} > \bar{C}^0_{\mathcal{B}}$ no $\mathcal{B}$ can escape, and the excess $\mathcal{A}$ accumulates at its pI.

These results can be transformed so as to apply to the inverse relationship between the isoelectric points, $pI_{\mathcal{C}} > pI_{\mathcal{A}} > pI_{\mathcal{B}}$, simply by rotating the patterns 180° about the center of the abscissa.

Reaction (2). The fundamental difference between reactions (1) and (2) is that in the latter case one of the reactants (namely, the ligand) is not amphoteric and has a constant velocity, at least over the pH range encompassing $pI_{\mathcal{P}}$ and $pI_{\mathcal{PL}}$. Consequently, their isoelectric focusing profiles are distinctly different. Focusing patterns for reaction (2) have been computed

for a range of values of the several parameters, the most provocative results being displayed in figs. 5 and 6. Let us first consider those obtained for $K_2 = 2 \times 10^6\,M^{-1}$, $V_{\mathcal{L}} = -2.5 \times 10^{-4}\,cm\,s^{-1}$ and $\bar{C}^0_{\mathcal{L}} = \bar{C}^0_{\mathcal{P}}$ (fig. 5A). The early transient patterns are bimodal with one of the peaks proximate to $pI_{\mathcal{P}}$ and the other roughly centered between $pI_{\mathcal{P}}$ and $pI_{\mathcal{PL}}$. As equilibrium is approached the proximal peak grows at the expense of the other peak until the pattern becomes unimodal so that eventually a single peak focuses at $pI_{\mathcal{P}}$. As shown in fig. 5B the proximal peak corresponds to essentially pure $\mathcal{P}$, while the other one contains all three species in chemical equilibrium and is, in fact, a somewhat overlapping reaction zone. As the electric field drives the ligand towards the anode and out of the focusing column, the concentration of ligand in the reaction zone decreases progressively; $\mathcal{PL}$ dissociates by mass action; and the $\mathcal{P}$ released from the complex is driven towards its pI. This acounts for the growth of the proximal peak with time. At equilibrium the column contains only unliganded $\mathcal{P}$ focused at its pI.

Similar results were obtained for $\bar{C}^0_{\mathcal{L}} = 10\bar{C}^0_{\mathcal{P}}$ and for $K_2 = 1 \times 10^6\,M^{-1}$; but bimodal transient patterns are not generated when $V_{\mathcal{L}} = -5 \times 10^{-4}\,cm\,s^{-1}$, because the ligand is driven out of the focusing column too rapidly. Nor do weaker interactions, $K_2 \leqslant 5 \times 10^5\,M^{-1}$, give bimodal patterns.

For much stronger interactions (e.g., $K_2 = 2 \times 10^8\,M^{-1}$) the two peaks in the transient patterns are very well resolved even when $V_{\mathcal{L}} = -5 \times 10^{-4}\,cm\,s^{-1}$ (fig. 5C). The reaction zone is located close to $pI_{\mathcal{PL}}$, since it contains a high concentration of $\mathcal{PL}$ relative to the concentrations of $\mathcal{P}$ and $\mathcal{L}$. Because the chemical equilibrium in the reaction zone is satisfied by concentrations of $\mathcal{P}$ and $\mathcal{L}$ which are about one and two orders of magnitude less than the concentration of $\mathcal{PL}$, respectively, relatively small amounts of reactants are driven out of the zone per unit time. Consequently, the approach to equilibrium is slower than for the weaker interaction of fig. 5A.

These results are for a narrow initial zone of material positioned cathodically to the pI's. When it is anodic to the pI's the transient patterns are still bimodal, but the path to equilibrium is different (compare fig. 6 with fig. 5A). For the earliest time shown in fig. 6, both peaks are in the vicinity of $pI_{\mathcal{PL}}$. As focusing proceeds and ligand is driven out of the column, the reaction zone decreases in size, remaining close to $pI_{\mathcal{PL}}$ while the growing peak of $\mathcal{P}$ migrates along the column to its pI. An intermediate type of behavior is exhibited when the system is focused from a broad initial zone.

Our calculations are for a negatively charged ligand, but the patterns transform to those for a positive ligand and $pI_{\mathcal{PL}} > pI_{\mathcal{P}}$ when rotated 180° about the center of the abscissa.

4. Discussion

The transient and equilibrium isoelectric focusing patterns for reaction (1), $pI_{\mathcal{A}} < pI_{\mathcal{C}} < pI_{\mathcal{CB}}$, find their counterparts in the density gradient sedimentation patterns computed by Kegeles et al. [17] for reaction (1) with $\mathcal{C}$ of intermediate density, when the volume of reaction is zero so that there is no pressure effect. (Compare fig. 1C with their fig. 5.) In a different vein, the focusing patterns for reaction (1), $pI_{\mathcal{A}} < pI_{\mathcal{C}} < pI_{\mathcal{CB}}$ or $pI_{\mathcal{C}} < pI_{\mathcal{A}} < pI_{\mathcal{CB}}$, are similar in shape to the transport patterns computed by Bethune and Kegeles [18] for the same reaction in counter-current distribution, but also applicable to partition chromatography and zone electrophoresis. Although the similarity is partly artifactual due to the reduced abscissal coordinates used to display the transport patterns, it is also so that some of the same principles apply. Consider, for example, the case of zone electrophoresis in which the electrophoretic mobility of $\mathcal{C}$, $\mu_{\mathcal{C}}$, is intermediate between the mobilities of $\mathcal{A}$ and $\mathcal{CB}$, $\mu_{\mathcal{CB}} < \mu_{\mathcal{C}} < \mu_{\mathcal{A}}$. For sufficiently large equilibrium constant, a single peak corresponding to $\mathcal{C}$ is observed during early stages of electrophoresis; but as the zone migrates along the column, three peaks develop, the peripheral ones corresponding to $\mathcal{A}$ and $\mathcal{CB}$. As electrophoresis proceeds, the peripheral peaks grow at the expense of the central one. This behavior can be understood in terms of dissociation of $\mathcal{C}$ via mass action in response to both the dilution which occurs during diffusional spreading of the central peak and the differential migration of the three species in which newly formed $\mathcal{CB}$ is left behind and $\mathcal{A}$ moves out ahead of $\mathcal{C}$. One would expect all of the $\mathcal{C}$ to dissociate eventually, in which limit the transport pattern would exhibit two peaks corresponding to the separated $\mathcal{A}$ and $\mathcal{CB}$. The point of these comparisons is that concepts elaborated for one method of

protein separation can often be adapted qualitatively to other methods. Thus, as discussed by Bethune and Kegeles [18] for transport methods, it is possible in isoelectric focusing to obtain information about bimolecular complex formation by varying the relative amounts of the reactants. As shown in figs. 1, 3 and 4 one can deduce whether the complex is of intermediate pI or is characterized by a lower or higher pI than both reactants.

The foregoing discussion pertains to the interaction between two macromolecules, but in practice one of the reactants might be an amphoteric ligand such as a small peptide. The same qualitative considerations would still apply. If, however, the ligand is non-amphoteric, distinctively different focusing profiles are predicted by the results for reaction (2). These results provide an explanation for the provocative observations of Righetti and Drysdale [12–19] on the isoelectric focusing of dihydrofolate reductase (species not given) and its complexes with substrate or coenzyme. The pure enzyme focuses as a single band with pI 6.5. A mixture of enzyme ($\mathcal{E}$) and dihydrofolate ($\mathcal{FH}_2$) shows two closely spaced bands, one corresponding to $\mathcal{E}$ and the other to the $\mathcal{E}$ - $\mathcal{FH}_2$ complex. A mixture of the enzyme and its coenzyme shows three bands corresponding to $\mathcal{E}$, $\mathcal{E}$-$\mathcal{NADP}^+$ and $\mathcal{E}$-$\mathcal{NADPH}$, both of the complexes being located in the vicinity of pH 4.0. (The bands were identified by tracer studies using radioactive substrate and coenzyme.) The patterns of the enzyme-ligand mixtures change with time, such that after prolonged electro-focusing they show only the band of $\mathcal{E}$. This is the kind of behavior predicted for reaction (2), but before drawing the comparison it is necessary to note that (1) dihydrofolate reductase binds its ligands strongly, $\mathcal{NADPH}$ more strongly than $\mathcal{FH}_2$ [‡1]; (2) the rates of association and dissociation of the $\mathcal{E}$ - $\mathcal{NADPH}$ are rapid [‡2] compared to the time of electrofocusing [‡3]; and (3) we estimate that the electrophoretic mobility of $\mathcal{NADPH}$ is about twice as large as for $\mathcal{FH}_2$. According, the experimentally observed behavior for the enzyme-substrate and enzyme-cofactor mixtures can be compared with the theoretical behavior shown in figs. 5A and 5C, respectively [‡4]. The agreement between theory and experiment is quite reasonable and, thus, lends confidence in the application of isoelectric focusing to the detection of specific interactions of enzymes and other proteins with ligands such as allosteric affectors and drugs.

The comparison also points up an important theoretical prediction; namely, in general the pI of a protein-ligand complex cannct be determined accurately using conventional focusing procedures. It can only be ascertained that the pI is equal to or greater than a certain value. In the accompanying communication [16] we formulate the theory of a procedure which permits determination of, not only the pI of such complexes, but more importantly, the intrinsic ligand-binding constant for weak as well as strong interactions.

[‡1] Values of the association constant for $\mathcal{FH}_2$ fall in the range 1.4×10^5 to 5×10^6 M^{-1} depending upon the species and apparently the pH [20–23]; for $\mathcal{NADPH}$, 2.6×10^5 to $>10^8$ [20–24]; and for $\mathcal{NADP}^+$, 8×10^4 to 1×10^6 M^{-1} [20–22,24].

[‡2] Binding of $\mathcal{NADPH}$ to dihydrofolate from a methotrexate-resistant strain of *L. Casei* takes place in two phases [24]: The faster characterized by an apparent bimolecular rate constant of about 10^7 M^{-1} s^{-1} at 25°C, the slower by a pH-dependent, unimolecular rate constant which varies from 0.06 to 0.012 sec^{-1}. The dissociation rate at pH 6 is 0.27 s^{-1}.

[‡3] It has been shown [25] that conclusions concerning the sedimentation behavior of associating-dissociating systems in the limit of instantaneous establishment of equilibrium are also valid for reactions characterized by half-times as long as 20–60 sec.

[‡4] Although Righetti and Drysdale [19] do not tell us whether in this particular instance the narrow initial zone of material was applied at the cathode or anode end of the focusing column, Drysdale [12] does say that it is generally preferable to apply samples at the cathode end. We presume that they have done so in the case of dihydrofolate reductase.

References

[1] J.R. Cann and D.I. Stimpson, Biophys. Chem. 7 (1977) 103.
[2] D.I Stimpson and J.R. Cann, Biophys. Chem. 7 (1977) 115.
[3] D.L. Hare, D.I. Stimpson and J.R. Cann, Arch. Biochem. Biophys. 187 (1978) 274.
[4] J.R. Cann, D.I. Stimpson and D.J. Cox, Anal. Biochem. 86 (1978) 34.
[5] R. Frater, J. Chromatogr. 50 (1970) 469.
[6] J.R. Yates, quoted by R. Frater, J. Chromatogr. 50 (1970) 469.
[7] K. Felgenhauer, D. Graesslin and B.D. Huismans, Prot. Biol. Fluids 19 (1971) 575.
[8] J.W. Drysdale and P. Righetti, Biochemistry 11 (1972) 4044.

[9] K. Wallevik, Biochim. Biophys. Acta 322 (1973) 75.
[10] P. Talbot, in: Isoelectric focusing, eds. J.P. Arbuthnott and J.A. Beeley (Butterworths, London, 1975) p. 270.
[11] E. Galante, T. Carvaggio and P.G. Righetti, Biochim. Biophys. Acta 442 (1976) 309.
[12] J.W. Drysdale, in: Methods of protein separation, Vol. 1, ed. N. Catsimpoolas (Plenum Press, New York, 1975) ch. 4.
[13] P.G. Righetti and J.W. Drysdale, Ann. N.Y. Acad. Sci. 209 (1973) 163.
[14] C.M. Park, Ann. N.Y. Acad. Sci. 209 (1973) 237.
[15] H. Rilbe, Ann. N.Y. Acad. Sci. 209 (1973) 80.
[16] R.J. Cann and K.J. Gardiner, Biophys. Chem. 10 (1978) 211.
[17] G. Kegeles, L. Rhodes and J.L. Bethune, Proc. Natl. Acad. Sci. USA 58 (1967) 45.
[18] J.L. Bethune and G. Kegeles, J. Phys. Chem. 65 (1961) 1755.
[19] P.G. Righetti and J.W. Drysdale, Ann. N.Y. Acad. Sci. 209 (1973) 163.
[20] J.P. Perkins and J.R. Bertino, Biochemistry 5 (1966) 1005.
[21] R.L. Blakley, The Biochemistry of folic acid and related pteridines (North-Holland, Amsterdam, 1969) ch. 5.
[22] J.G. Dann, G. Ostler, R.A. Bjur, R.W. King, P. Scudder, P.C. Turner, G.C.K. Roberts and A.S.V. Burgen, Biochem. J. 157 (1976) 559.
[23] A.V. Leddy, W.D. Behnke and J.H. Freisheim, Biochem. Biophys. Acta 533 (1978) 415.
[24] S.M.J. Dunn, J.G. Batchelor and R.W. King, Biochemistry 17 (1978) 2356.
[25] J.R. Cann and G. Kegeles, Biochemistry 13 (1974) 1868.